SOFTWARE RAKE RECEIVER ENHANCED GPS SYSTEM

Daniel Iancu[*], John Glossner[†,*], Hua Ye[*], Mayan Moudgill,[*] and Vladimir Kotlyar[*,]

[*]Sandbridge Technologies, Inc.
1 North Lexington Ave.
White Plains, NY 10601 USA
{diancu, jglossner , huaye, mayan, vkotlyar}@SandbridgeTech.com

[†]Delft University of Technology
Computer Engineering
Electrical Engineering, Mathematics and Computer Science
Delft, The Netherlands

ABSTRACT

Acceleration of semiconductor technologies has enabled incorporation of GPS receivers in small inexpensive hand held battery operated devices. As the size of chipsets for different communication protocols diminishes in size, building multi-protocol communication systems including GPS receivers has become not only attractive but also possible. A limitation of current approaches requires the Baseband (BB) processor to be implemented with hardware. Furthermore, if advanced techniques such as Rake receivers are desired to improve reception over multiple paths, significant additional hardware may be required. This presents both size and cost issues. In this paper we extend our work previously presented [1] by describing results for reflective environments by using a Rake receiver. The baseband processing, including the Rake receiver, is implemented entirely in software, using the Sandbridge Technologies™ Sandblaster™ Digital Signal Processor (DSP) platform. An advantage of a software approach is that differing algorithms may utilized in various environments. Using our software implementation we show that the link margin may be improved by 3dB using the Rake receiver.

INTRODUCTION

A GPS constellation consists of 24 active satellites placed on 6 orbits with 4 symmetrically placed satellites per orbit [2][3]. The satellites are controlled and monitored by a network of fixed terrestrial stations. The terrestrial stations upload navigation and control data information on a timely basis. The stations also monitor the satellites' status and health. All satellites carry a very accurate atomic clock that is synchronized to the satellite system clock[4]. All satellites synchronously broadcast navigation and ranging data using a Direct Sequence Spread Spectrum (DSSS) protocol using different carrier frequencies called L1 (1575.42 MHz) and L2 (1227.6 MHz). The L1 band is dedicated for commercial use while the L2 band is reserved for military applications. On the L1 band each satellite transmits on the same frequency using a different 1023 long Pseudo Random Number (PRN) sequence spreading code. There are 32 PRN codes and each satellite has allocated a PRN sequence. The number of the PRN sequence is in fact the satellite ID.

Since the GPS system supports only one way transmission, from the satellites to the user, there are an unlimited number of possible users receiving the signal from all visible satellites. At one geographical location there are maximum 12 visible satellites at a time.

All satellites simultaneously transmit the navigation data. The navigation data from one satellite includes the satellite ephemeris and the satellite constellation almanac data at the moment when the transmission starts.

The ephemeris data is used by the GPS receiver to determine the satellite position with very high accuracy, while the ranging code is used to measure the time elapsed between the time of transmission and the time of reception called Time of Arrival (TOA). Since the receiver time is not synchronized to the satellite system time there is an unknown error in the propagation time measurement. Therefore, in order to measure the location, latitude, longitude and height, the receiver needs to measure the ranging signal from four satellites. By solving a system of four equations with four unknowns, the receiver will be able to find its own location referenced to the center of the earth and the TOA measurement error [5]. .

The GPS receiver faces two major design challenges. First, the GPS power level at the surface of the earth is very low. For the L1 band the power level is not expected to exceed -157 dBW. Second, the satellites period of rotation is approximately 43080 seconds or 11 hr and 58 min, resulting in Doppler shifts of several KHz. In a spread spectrum system the lower the signal strength the longer is the required correlation time for signal detection. On the other hand, the correlation time cannot be longer than the coherence time, therefore the GPS receiver must compensate for the Doppler shift while correlating the received signal with the PRN code.

Usually, in the receiver, there is one dedicated hardware block for each tracked satellite called a channel. Each channel includes correlation, Doppler frequency correction and synchronization units.

The presence of multi-path propagation will further impair the integrity of the received signal and consequently the TOA measurement. The ranging

measurement errors result in significant positioning errors. Therefore, in a multi-path propagation situation a Rake Receiver structure [6] may help to combine the power from multiple paths and bring the overall signal to detectable levels. Unfortunately, for each Rake Receiver finger one more channel needs to be allocated because the demodulator is timed to a different chip position. This may require significant additional hardware.

To keep the Dilution of Precision (DOP) low [7][8] (e.g. to minimize the positioning errors), more than four satellites must be tracked at a time resulting in even more channels required. The number of channels in a GPS receiver will directly impact the silicon area requirements and consequently impact the cost of the receiver.

In current GPS designs, most of the physical layer is implemented using dedicated hardware blocks with the size of the used silicon area proportional to the number of channels, giving little flexibility and scalability.

In contrast, a software implementation provides flexibility and scalability and may be dynamically configured as dictated by the mode of operation and the propagation conditions within a changing environment.

In the following we present the theoretical foundation and the software implementation of a GPS receiver that is real-time reconfigurable to meet different modes of operation and precision of positioning criteria with no extra hardware added and also coexisting with other wireless communication protocols.

THEORY OF OPERATION

Signal Model

At the receiver side, the GPS signal is a superposition of DSSS signals coming from all visible satellites each with shifted carrier frequency due to the Doppler Effect and, specific PRN signature. For the Coarse Acquisition (C/A) code [1] the received signal without multi-path reflections can be modeled as

$$s(t)=\sum_{i=0}^{N_s-1}\sum_{n=-\infty}^{+\infty}\sum_{k=-\infty}^{+\infty}A_i d_i[k]g\left(t-k\frac{N_p}{f_i}\right)g\left(t-n\frac{1}{f_i}\right)\times \quad (1)$$
$$\times P_i[(n+n_i^{'})\%N_p]\cdot\cos(2\pi f_i t+\varphi_i)$$

where the noise and in-band interference terms have been deliberately ignored for readability.

The information conveyed by a specific satellite can be extracted by performing the following mathematical operations on Equation (1):

Multiplication by

$$g\left(t-k^{'}\frac{N_p}{f}\right)\cdot g\left(t-m\frac{1}{f}\right)\cdot\cos(2\pi f\ t)$$

Multiplication by

$$-j\cdot g\left(t-k^{'}\frac{N_p}{f}\right)\cdot g\left(t-m\frac{1}{f}\right)\cdot\sin(2\pi f\ t),$$

Addition of the two previous expressions

$$\chi(t)=s(t)\cdot g\left(t-k^{'}\frac{N_p}{f}\right)\cdot g\left(t-m\frac{1}{f}\right)\times$$
$$\times\cos(2\pi f\ t)-s(t)\cdot j\cdot g\left(t-k^{'}\frac{N_p}{f}\right)\times$$
$$\times g\left(t-m\frac{1}{f}\right)\cdot\sin(2\pi f\ t)=$$
$$=\sum_{i=0}^{N_s-1}\sum_{n=-\infty}^{+\infty}\sum_{k=-\infty}^{+\infty}\xi_{i,k,n}\cdot g\left(t-k^{'}\frac{N_p}{f}\right)g\left(t-k\frac{N_p}{f_i}\right)\times$$
$$\times g\left(t-m\frac{1}{f}\right)g\left(t-n\frac{1}{f_i}\right)\cdot\cos(2\pi f_i t+\varphi_i)e^{-j2\pi ft} \quad (2)$$

where, $j=\sqrt{-1}$, f is the carrier frequency at the transmitter and is the same for all satellites, and

$$\xi_{i,k,n}=A_i d_i[k]P_i[(n+n_i^{'})\%N_p]$$

Without losing generality, f can be viewed as the Local Oscillator (LO) frequency, equal to the receiver IF frequency. In Equation (2) the product of pulse functions

$$g\left(t-k^{'}\frac{N_p}{f}\right)\cdot g\left(t-m\frac{1}{f}\right)\cdot g\left(t-k\frac{N_p}{f_i}\right)\cdot g\left(t-n\frac{1}{f_i}\right)$$

will be different from zero only if $k=k^{'}$ and $m=n$. This means that for a specified $k=k'$ and $m=n$, on a time scale, it will be a single chip selected, as illustrated in Figure 1.

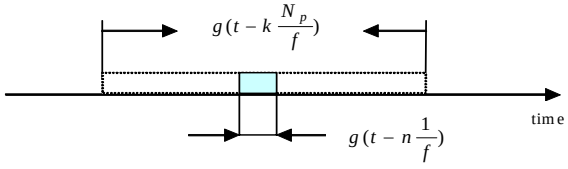

Figure 1 *GPS chip selection showing the highlighted part as the only non zero part over time in equation (2).*

After summation, Equation (2) becomes

$$\chi(t) = \sum_{i=0}^{N_s-1} A_i d_i[k] P_i[(n+n_i^{'})\%N_p] \cdot \cdot g\left(t - n\frac{1}{\max(f, f_i)}\right)\cos(2\pi f_i t + \varphi_i)\cdot e^{-j2\pi ft} \quad (3)$$

The integral of $\chi(t)$ over the entire time axis represents the Fourier transform of $\cos(2\pi f_i t + \varphi_i)$ times a constant:

$$\int_{-\infty}^{+\infty} \chi(t)dt = \int_{n\cdot T}^{(n+1)\max(T,T_i)} \chi(t)dt = \int_{n\cdot T}^{(n+1)\cdot\max(T,T_i)} dt \sum_{i=0}^{N_s-1} A_i d_i[k] P_i[(n+n_i^{'})\%N_p]\cdot\cos(2\pi f_i t+\varphi_i)\cdot e^{-j2\pi ft} =$$
$$= \int_{n\cdot T}^{(n+1)\cdot\max(T,T_0)} dt \quad A_o d_0[k] P_0[(n+n_0^{'})\%N_p]\cdot\cos(2\pi f_0 t+\varphi_0)\cdot e^{-j2\pi ft} +$$
$$+ \int_{n\cdot T}^{(n+1)\cdot\max(T,T_1)} dt \quad A_1 d_1[k] P_1[(n+n_1^{'})\%N_p]\cdot\cos(2\pi f_1 t+\varphi_1)\cdot e^{-j2\pi ft} + \ldots$$
$$+ \int_{n\cdot T}^{(n+1)\cdot\max(T,T_{N_s-1})} dt \quad A_{N_s-1} d_{N_s-1}[k] P_{N_{s-1}}[(n+n_{N_s-1}^{'})\%N_p]\times$$
$$\times\cos(2\pi f_{N_s-1}t+\varphi_{N_s-1})\cdot e^{-j2\pi ft} \quad (4)$$

For the positive frequencies of a single satellite, after integration, Equation (4) becomes

$$D_i(k,n+n_i^{'}) \int_{nT}^{(n+1)\cdot\max(T,T_i)} dt \cdot\cos(2\pi f_i t+\varphi_i)\cdot e^{-j2\pi ft} =$$
$$D_i(k,n+n_i^{'})\cos\varphi_i \int_{n\cdot T}^{(n+1)\cdot\max(T,T_i)} dt \cdot\cos(2\pi f_i t)\cdot e^{-j2\pi ft} -$$
$$- D_i(k,n+n_i^{'})\sin\varphi_i \times$$
$$\times \int_{n\cdot T}^{(n+1)\cdot\max(T,T_i)} dt \cdot\sin(2\pi f_i t)\cdot e^{-j2\pi ft} =$$

$$= D_i(k,n+n_i^{'})\cos\varphi_i \int_0^T dt\cdot\cos(2\pi f_i t)\cdot e^{-j2\pi ft} -$$
$$- D_i(k,n+n_i^{'})\sin\varphi_i \int_0^T dt\cdot\sin(2\pi f_i t)\cdot e^{-j2\pi ft} +$$
$$+ D_i(k,n+n_i^{'})\cos\varphi_i \int_T^{T_i} dt\cdot\cos(2\pi f_i t)\cdot e^{-j2\pi ft} -$$
$$- D_i(k,n+n_i^{'})\sin\varphi_i \int_T^{T_i} dt\cdot\sin(2\pi f_i t)\cdot e^{-j2\pi ft} =$$
$$= \frac{D_i(k,n+n_i^{'})\cos\varphi_i}{2}\delta(f-f_i) +$$
$$j\frac{D_i(k,n+n_i^{'})\sin\varphi_i}{2}\delta(f-f_i) + E_i \quad (5)$$

where $A_i d_i[k] P_i[(n+n_i^{'})\%N_p] = D_i(k,n+n_i^{'})$ and

$$E_i = D_i(k,n+n_i^{'})\cos\varphi_i \int_T^{T_i} dt\cdot\cos(2\pi f_i t)\cdot e^{-j2\pi ft} -$$
$$- D_i(k,n+n_i^{'})\sin\varphi_i \int_T^{T_i} dt\cdot\sin(2\pi f_i t)\cdot e^{-j2\pi ft}$$

In the previous formula, E_i represents the error introduced by windowing.

Summing for all visible satellites Equation (5) yields

$$\sum_{i=0}^{N_s-1}\int_{-\infty}^{+\infty}\chi(t)dt = \sum_{i=0}^{N_s-1}\frac{D_i(k,n+n_i^{'})\cos\varphi_i}{2}\delta(f-f_i) +$$
$$+ j\frac{D_i(k,n+n_i^{'})\sin\varphi_i}{2}\delta(f-f_i) + \sum_{i=0}^{N_s-1} E_i \quad (6)$$

In Equation (6), if $f - f_i = 0$ and $\varphi_i = 0$, the imaginary term and the sum of errors will vanish. The only term remaining is the first sum representing the data transmitted by the satellites.

The result is that in order to correctly demodulate the signal coming from different satellites, one needs to correct for both phase and frequency for each satellite.

IMPLEMENTATION

Currently, the most common implementations for GPS receivers use dedicated hardware blocks. A simplified system block diagram for a generic GPS receiver is shown in Figure 2. The RF signal after conditioning and down conversion is digitized and processed by a base band processor. The navigation and ranging data are uploaded to a DSP/RISC processor and further processed to obtain the position.

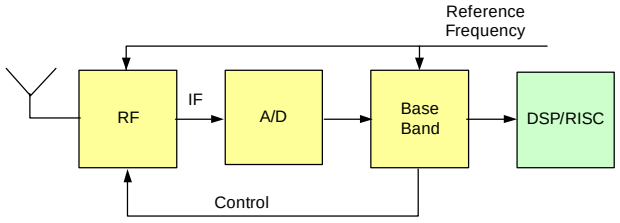

Figure 2 *GPS system block diagram for H/W implementation.*

The baseband block in Figure 2 includes all the necessary hardware for carrier frequency synchronization, frequency phase and code tracking, and data demodulation for each satellite. This means that for each satellite there is one channel allocated (although sometimes one channel can be multiplexed between two satellites) to track and compensate for the frequency and phase shift and track the PRN code.

The receiver frequency tracking and code tracking block diagrams are depicted in Figure 3 and Figure 4. A detailed description of the carrier frequency and code tracking can be found in [9].

In Figure 3, a digital IF signal is multiplied by a sine-cosine table and correlated with the PN sequence to obtain the digital I and Q signals. The output of the loop discriminator is filtered and fed to a numeric control oscillator which provides the advance or delay of the sin-cosine output table. In H/W implementations there are multiple replicas of this circuit, one per tracked satellite.

The PRN code is typically tracked using an early-late circuit. The output of the code loop filter, controls the timing (advance or delay) of the PRN code generator. In H/W implementations there are typically multiple replicas of this circuit, one per tracked satellite.

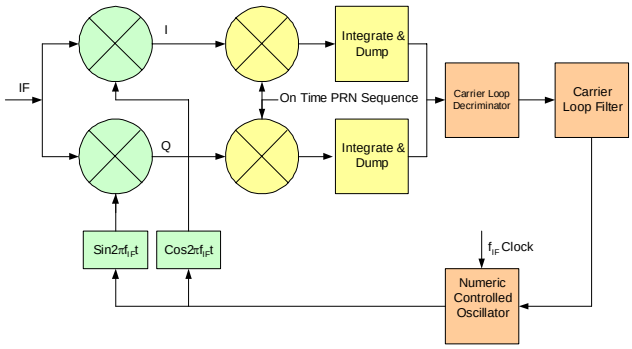

Figure 3 *H/W implementation; block diagram for receiver carrier tracking*

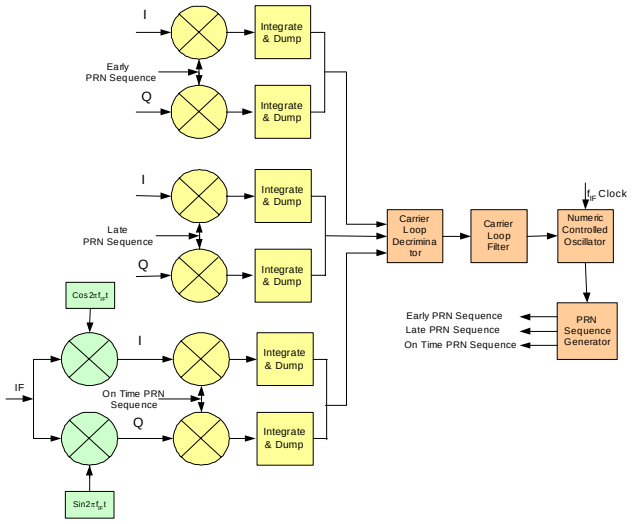

Figure 4 *H/W implementation block diagram for receiver code tracking*

In our software implementation the frequency and code tracking are implemented using a different methodology. The frequency shift information is determined using time domain analysis. It is performed as follows. The data resulting from sampling the IF frequency over a certain predefined time interval is stored in a buffer. The data in the buffer is then multiplied with a sine-cosine table. Instead of controlling the phase of the sine-cosine table in order to compensate for the carrier frequency shift, the buffered data is time domain shifted by pointer manipulation. The pointer is advanced or delayed depending on the direction of the Doppler shift. The sine-cosine table will be the same for all carrier frequencies.

The phase information is determined by employing a digital PLL executed also in software. Depending on the PLL output, an additional shift on the already shifted data may be required. The effect of the shifting data in the time domain is to create

spurious frequencies in the frequency domain which results in detection errors. On a pure sine waveform the effect of the shifting is shown in Figure 5. It can be shown that the detection error converges to zero as $\frac{1}{N^2}$, where *N* is the number of over-samples per IF cycle. The shift on the PRN sequence is achieved also through pointer manipulation since all 32 PRN sequences are stored in memory.

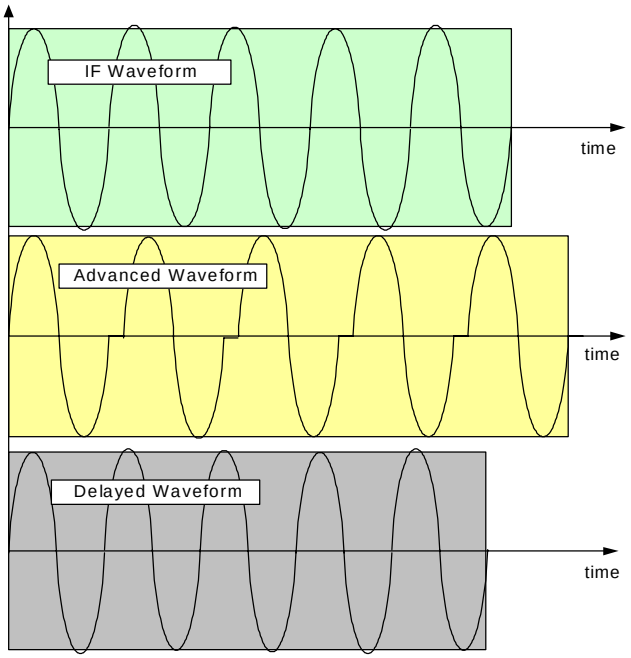

Figure 5 *Waveform distortion by advancing or retarding the IF data*

The main S/W blocks for baseband processing are illustrated in Figure 6. The buffered IF data after filtering, shifting, and interpolation is multiplied with the sin-cosine table and integrated over one IF cycle period. After correlation with the PRN sequence the I and Q data take two different paths, one is to the upper layer to process the navigation data and the second is for further base band processing for sky search, synchronization, and tracking.

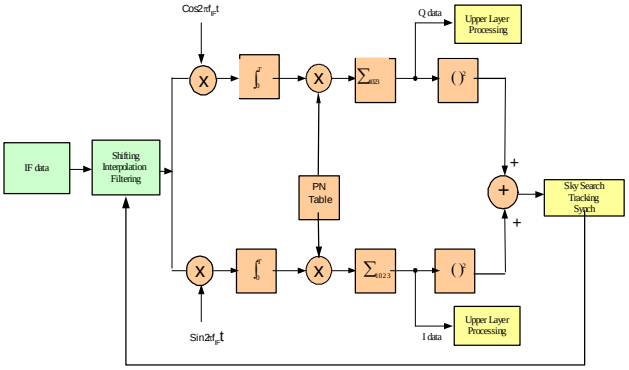

Figure 6 *Receive S/W implementation base band block diagram*

Shifting, Filtering and Interpolation

The blocks in Figure 7 provide the means to shift the IF data one sample at a time every n samples conforming to a specific Doppler bin. They also perform an extra sample shift according to the digital PLL output to keep the PLL locked. Sample interpolation as required by the Delay Locked Loop (DLL) output to improve the TOA accuracy is also performed. In addition an FIR shaping filtering is implemented to improve the receiver performance. Demodulation is performed on the already shifted data using a sine-cosine lookup table with N_{OVS} samples per cycle. The integration over N_{OVS} samples provides one I/Q sample decimated N_{OVS} times. The correlation with the PRN sequence provides one data sample. The I/Q data is subsequently processed based on the intended function (e.g. Satellite search, I^2+Q^2, PLL, IxQ, DLL, I^2+Q^2, or De-spreading Q).

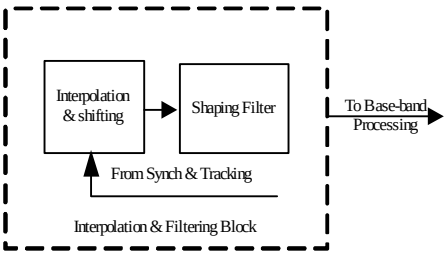

Figure 7 *Interpolation, shifting and filtering block.*

Sky search

The process of detecting the visible satellites is called sky search. If there is no previous knowledge of the satellite constellation at a given time and location, the search for the visible satellites becomes a compute intensive process because of the spread of the Doppler shifted carriers over several kHz. In this case the search is exhaustive over the entire Doppler frequency range as well as PRN range. The Doppler frequency range is divided into Doppler bins,

usually 50Hz wide; the search is performed for each Doppler bin and each PRN sequence. If the satellite constellation is known, the search is restricted to just a few Doppler bins and PRN sequences resulting in much less computational load.

To perform the search, the I and Q outputs from the demodulator, are correlated with a 1023 length PRN sequence at one sample per chip. These are squared and accumulated over several milliseconds and compared against a predetermined threshold. If it is above the threshold, the de-spreading process begins with the maximum correlation sample position. The data is collected for the length of a subframe and is searched for the preamble [1]. If the preamble is found then the search is successful and the visible satellite list is updated.

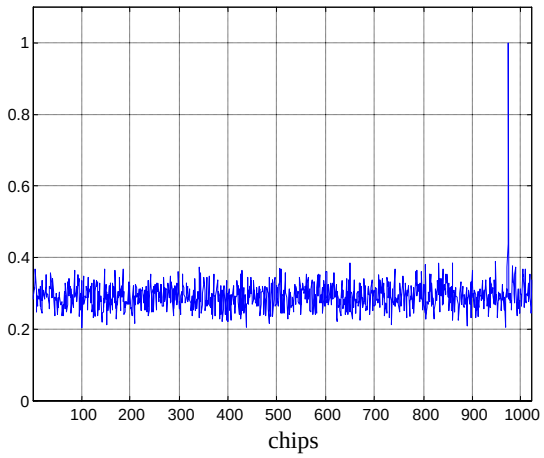

Figure 8 *Satellite search, cross correlation output for PRN 1, 6 satellites in view, -30 dB SNIR.*

Figure 8 illustrates the search for a constellation of six satellites all at equal power and -30 dB signal to noise and interference ratio (SNIR). The satellite is successfully identified at 980 chips.

Synchronization and Tracking.

The two major blocks for synchronization and tracking are the digital PLL and DLL, also entirely implemented in S/W in our system.

Digital PLL

The digital PLL block diagram is shown in Figure 9 . The PLL input consists of I and Q outputs where each output is limited to the three values -1, 0, or +1. A +1 output means advance one sample, 0 means do not shift and a -1 output means delay one sample.

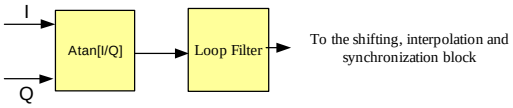

Figure 9 *Digital PLL block diagram.*

Figure 10 shows the accumulated errors in the shifting process. The data cannot be properly decoded without the digital PLL running. As the digital PLL is turned ON, the decoded data sequence {+1, -1, +1, -1,} can be easily seen in Figure 11.

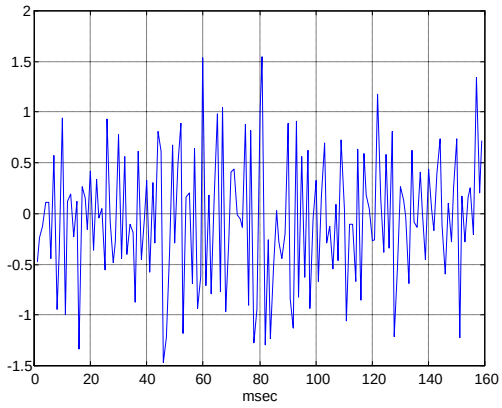

Figure 10 *Decoded data, Doppler shift 25 Hz, PLL turned OFF, SNIR -31 dB.*

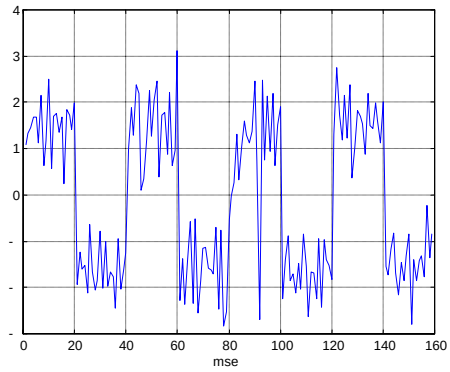

Figure 11 *Decoded data sequence {+1, -1, +1, -1, …}; Doppler shift 25 Hz, PLL turned ON, SNIR -31 dB.*

Digital DLL

The role of the digital DLL is to detect the subframe boundary at sub-chip resolutions to improve the positioning accuracy. The block diagram of the digital DLL is shown in Figure 12. The two identical branches in the block diagram execute the same function, with an

early and late replica of the PRN sequence, advanced and delayed by a half chip respectively. The I and Q data from the demodulator is correlated with the early and late versions of the PRN sequence, it is then squared and subtracted as described by

$$(I_e^2 + Q_e^2) - (I_l^2 + Q_l^2)$$

where : I_e , I_l , Q_e , Q_l are the early and late I and Q .

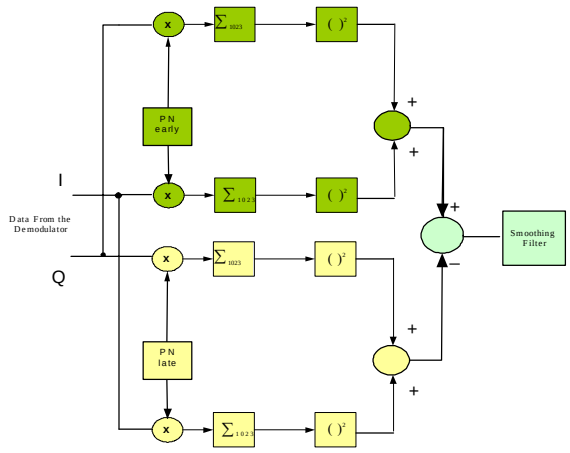

Figure 12 *Digital DLL block diagram.*

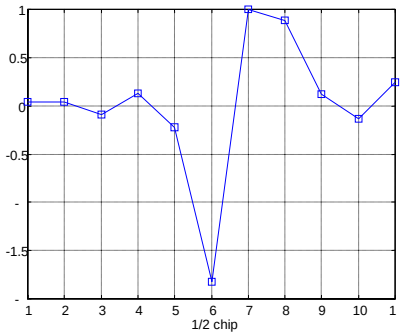

Figure 13 *Output of the digital DLL.*

The filtered output is shown in Figure 13. The minimum and maxima correspond to the early and late correlations. The subframe boundary is marked by the x axis intercept positioned between two chips. The more accurate frame boundary provides a more accurate TOA for the incoming sub-frames, and ultimately a more accurate user position estimate.

Multi Path Mitigation

In case of multi-path propagation, a common technique in DSSS is to use a Rake receiver. The rake receiver can improve substantially the signal detection level but at the expense computational complexity. For the GPS receiver, each path requires one more channel allocated to that specific satellite. In hardware the number of channels are limited to the performance/cost structure of the receiver giving little flexibility, if any at all, to the end user in multi-path propagation conditions. In our software approach, adding the Rake receiver is only limited by the available computational capacity of the platform. As an example, if the processor is idle except for GPS processing, the entire platform may be allocated to the GPS receiver with computationally complex algorithms.

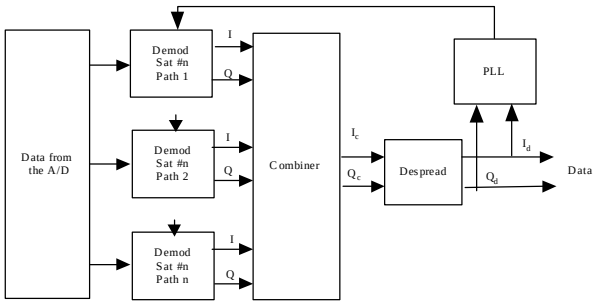

Figure 14 *Rake Receiver structure.*

The Rake receiver block diagram employed is given in Figure 14, [12][13]. For each path there is one more channel, or Rake Receiver finger added, and the output of each channel is combined and de-spread. The output from the de-spread block is further processed by the PLL for synchronization purposes and also by the upper layer.

Figure 15 illustrates the search result for multi-path propagation with the first two paths at the same power level and two more paths both at a 3dB lower power level.

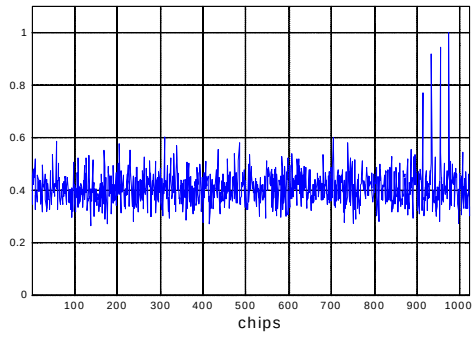

Figure 15 *Satellite search result for PN#1, with 6 satellites in view, with total SNIR=-36dB. The 2nd path of equal power is ten chips away from the main peak.*

For a data sequence {1,-1,1,-1…}, without a Rake receiver, the detected data is illustrated in Figure 16. It can be seen that an error at the end of the sequence occurs. If a Rake receiver with two fingers is used, then the data is detected correctly as depicted in Figure 17.

The performance of the GPS Rake receiver using three fingers for one tracked satellite and one finger for

the rest of the tracked satellites is shown in Figure 18. The link margin improvement as a result of combining three paths as function of the 3rd path power referenced to the main path is shown for the case where the first two paths are kept at fixed power levels.

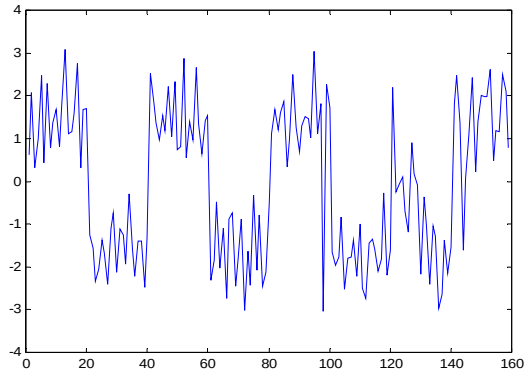

Figure 16 *Despreaded data using a single path*

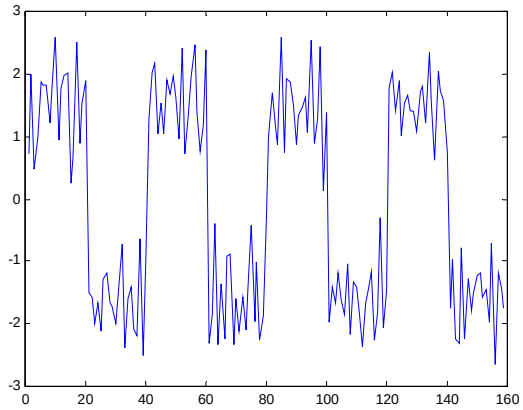

Figure 17 *Recovered data using a Rake receiver with two path combination.*

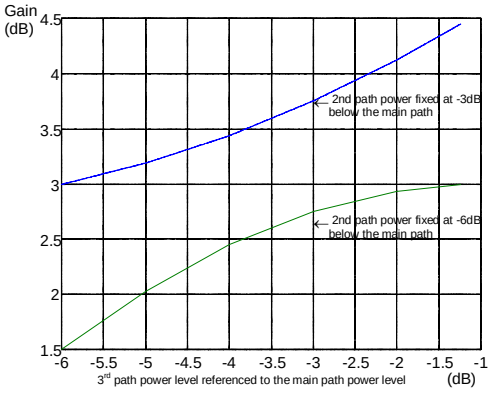

Figure 18 *Link margin improvement with a Rake receiver combining 3 paths*

SYSTEM DESIGN

The system platform used for implementation is shown in Figure 19. The RF signal is down converted first to an intermediate frequency IF and then to a Low IF. The reference frequency for the fractional PLL is provided by a high precision low drift crystal oscillator. The fractional PLL provides the input frequency to the RF, mixer and the A/D. The Sandblaster processor reads and controls the A/D, performs the Automatic Gain Control (AGC) function in software, provides the AGC control signal and also controls the PLL.

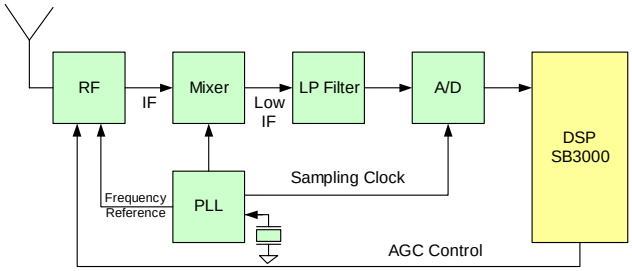

Figure 19 *H/W block diagram*

SANDBRIDGE IMPLEMENTATION

The baseband processing described in Figure 6 must be performed for each tracked satellite. In our S/W implementation it is possible to perform this in parallel because of the multithreaded processor. In a multithreaded environment, all the integrals in (6) are executed in parallel. The number of channels is dynamically allocated by the processor based upon the available resources and/or real time criteria.

Some heavily computational functions such as the sky search do not require real-time processing. In this case, to keep synchronization, the time is tracked using a high resolution timer, driven by a high accuracy crystal oscillator, such that the next buffer of data is precisely aligned in time.

All baseband processing for the GPS receiver has been implemented on the Sandbridge Sandblaster SB3000 multithreaded platform [10][11]. The performance for different positioning precision is shown in Figure 20. The receiver performance has been characterized for various update periods. For high accuracy with fast response (i.e. 5 meters and 100msec update response), about 1200MHz of processing is required. This is about half of the available capacity of a SB3000 chip. For more typical conditions (i.e. 75 meters and 500msec update response), only 400MHz of processing is required. This equates to about 15% utilization of the SB3000 platform.

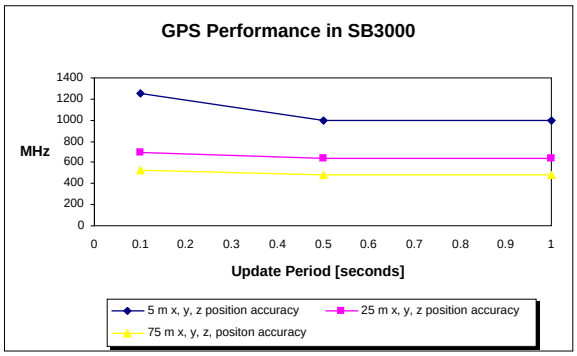

Figure 20 *GPS receiver performance under traditional environmental characteristics*

Figure 21 shows the GPS performance requirements for the same parameters as Figure 20 with the additional processing being the result of adding Rake processing to one of the satellites. This provides better reception in multipath environments at the expense of additional computational complexity.

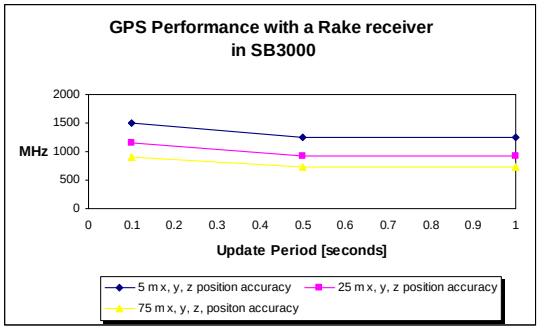

Figure 21 *GPS receiver performance using Rake techniques in reflective environments*

SUMMARY

We have presented a GPS receiver design implemented entirely in software that is capable of scalable and selectable performance characteristics over a number of environments. In high SNIR environments, traditional implementations of GPS receivers provide tradeoffs between computational capacity and location accuracy. In highly reflective and harsh SNIR environments, Rake receiver techniques may be employed that provide better characteristics at higher computational complexity. All GPS software is implemented on the Sandbridge Sandblaster platform as part of a multi-protocol communications handset component.

REFERENCES

[1] D. Iancu, J. Glossner, V. Kotlyar, H. Ye, M. Moudgill, and E. Hokenek, "Software Defined Global Positioning Satellite Receiver", *Proceedings of the 2003 Software Defined Radio Technical Conference (SDR'03)*, HW-2-001, 6 pages, Orlando, Florida, 2003.

[2] Global Positioning System Standard Positioning Service Signal Specification**,** *GPS NAVSTAR 2nd Edition, June 2*, 1995

[3] Elliot D. Kaplan, Understanding GPS Principles and Applications, *Artech House Inc. 1996.*

[4] Langley, R., Time, Clocks, and GPS, GPS Magazine, Advanstar, *Advanstar Communications*, Nov. / Dec.1991, pp.38-42.

[5] Bancroft, S., An Algebraic Solution of the GPS equations, *IEEE Trans. Aerospace and Electronic Systems*, Vol. AES-21 No 7, January 1985, pp. 56-59.

[6] J. Glossner, D. Iancu, J. Lu, E. Hokenek, and M. Moudgill, "A Software Defined Communications Baseband Design", *IEEE Communications Magazine*, Vol. 41, No. 1, pp. 120-128, Jan., 2003.

[7] DOD, NAVSTAR GPS User Equipment Introduction (Public Release Version), GPS Joint Program Office, Feb. 1991.

[8] Taylor & Francis Group, Mapping Dilution of Precision (MPOD) and map-matched GPS, *Int. J. Geographical Science*, 2002, vol. 16, No. 1, pp55-67.

[9] S. Haykin, Communication Systems, *John Wiley Sons. Inc*. 1983.

[10] J. Glossner, E. Hokenek, and M. Moudgill, Multithreaded Processor for Software Defined Radio, *SDR Forum Conference*, November, 2002, San Diego, CA.

[11] J. Glossner, S. Dorward, S. Jinturkar, M. Moudgill, E. Hokenek, M. Schulte, and S. Vassiliadis, Sandbridge Software Tools, *Proceedings of the 3rd International Worksop on Systems, Architectures, Modeling, and Simulation (SAMOS'03)*, July 21-23, 2003, pp. 142-147, Samos, Greece.

[12] Theodore S. Rappaport, "Wireless Communications", Prentice Hall Inc., 2002

[13] *E. Prince and P. Green,* A Communication Technique for Multipath Channels, *Proceeding of IRE, 1958.*

[14] E. O. Bringham, The Fast Fourier Transform And Its Applications, *Prentice-Hall Inc. 1988.*

[15] J. Glossner, E. Hokenek, and M. Moudgill, "Wireless SDR Solutions: The Challenge and Promise of Next Generation Handsets", *Accepted for publication at the 2002 Communications Design Conference*, September 2002, San Jose, CA.